RESTRICTED INVESTIGATION REPORT 1571R

CSIRO

INSTITUTE OF ENERGY AND EARTH RESOURCES

DIVISION OF MINERAL PHYSICS

INTRINSIC MAGNETIC PROPERTIES OF PYRRHOTITE

D.A. CLARK

P.O. Box 136

NORTH RYDE, NSW

AUSTRALIA 2113

FEBRUARY, 1985

TABLE OF CONTENTS

LIST OF TABLES

LIST OF FIGURES

INTRINSIC MAGNETIC PROPERTIES OF PYRRHOTITES

1 Magnetic Structure of Pyrrhotites

The ferrimagnetism of Fe_7S_8 (4C monoclinic pyrrhotite) was first adequately explained by Néel (1953) on the basis of the crystal structure proposed by Bertaut (1953). The detailed structure is depicted in Fig. 1. The magnetic moments of Fe atoms are parallel within each Fe layer but the sense of the magnetic moments alternates from layer to layer due to interlayer antiferromagnetic coupling.

In the absence of vacancies both iron sublattices (the even and odd Fe layers) are complete and possess equal and opposite magnetic moments. Thus stoichiometric FeS is antiferromagnetic. On the other hand, 4C pyrrhotite has inequivalent Fe sublattices due to the ordering of the vacancies onto alternate Fe layers, producing an uncompensated moment (ferrimagnetism), as shown in Fig. 2.

Because the spin ordering scheme described above (termed Type I ordering of a layer structure) applies to the pyrrhotite group as a whole the magnetic properties are determined by the distribution of vacancies. Structures with no vacancies (troilite) or disordered vacancies (1C pyrrhotite) are antiferromagnetic, whereas structures with vacancies confined to a single sublattice (4C and 3C superstructures) are ferrimagnetic. Other superstructures with ordered or statistically ordered vacancies, such as 5C and 6C pyrrhotites, are antiferromagnetic because the vacancies overall are equally distributed on both magnetic sublattices. For 6C pyrrhotite this equivalence is apparent from Fig. 2.

At room temperature the spins and the nett magnetic moment for 4C pyrrhotite lie within the basal plane, whereas for FeS the spins lie along the c-axis. Compositions close to stoichiometric FeS undergo a Morin or spin-flip transition at a temperature, T_s, which is composition dependent. $T_s \simeq 170^{\circ}C$ for FeS and decreases linearly with increasing x, by $150^{\circ}C$ per 1% Fe deficiency, so that $T_s \simeq 20^{\circ}C$ for $Fe_{0.96}S$ and $T_s \simeq -100^{\circ}C$ for $Fe_{0.93}S$ (Horwood et al., 1976).

For historical reasons the Néel point in the $Fe_{1-x}S$ system is referred to as the β-transition (it was originally confused with the vacancy disordering temperature). In the composition range FeS-Fe_7S_8 the Néel temperature is $\sim 325^{\circ}C$, (Haraldsen, 1941a; Hirone et al., 1954; Sparks and Komoto, 1964; Krasnicki et al., 1964; Andresen and Torbo, 1967).

A triad domain structure of FeS was deduced from Mössbauer studies by Horita and Hirahara (1971). In monoclinic pyrrhotite the triad domain structure (Besnus, 1966) is associated with structural twinning, whereas in FeS above T_s the spins lie in the basal plane and an antiferromagnetic domain structure consistent with the hexagonal crystal symmetry forms platy domains parallel to the basal plane, stacked along the c-axis, separated by 120° antiferromagnetic domain walls.

Many workers have studied the composition dependence of magnetic susceptibility and saturation magnetisation of $Fe_{1-x}S$.

Results from synthetic preparations (e.g. Haraldsen, 1941a, 1941b; Lotgering, 1956; Hihara, 1960; Perthel, 1960; Schwarz and Vaughn, 1972) and natural pyrrhotites (e.g. Hayase et al., 1963; Takeno, 1966; Besnus, 1966; Vaughn et al.,

(1971) establish that monoclinic 4C pyrrhotite is the only stable phase which possesses spontaneous magnetisation at room temperature. The spontaneous magnetisation is a maximum at the composition Fe_7S_8, for which $J_s \simeq 20$emu/g (92G). Pyrrhotite assemblages with lower values of J_s are mixtures of antiferromagnetic phases which have $0 \leq x \leq 0.1$ (FeS-Fe_9S_{10}) with ferrimagnetic pyrrhotite, for which $x \simeq 0.125$ (Fe_7S_8). This statement must be qualified, however, with the rider that metastable ferrimagnetic phases with other compositions, such as Fe_9S_{10}, can be formed in the laboratory by quenching from $\sim 200^{\circ}C$.

2 Exchange interactions in pyrrhotites

Fe atoms in the NiAs structure are too far apart for direct exchange interaction to occur, so magnetic ordering is accomplished by indirect coupling via sulphur atoms. Pyrrhotites exhibit strong antiferromagnetic coupling between layers with weaker coupling within layers. Consideration of the NiAs structure (Fig. 3) suggests that intralayer coupling in FeS involves 6 nearest neighbours whereas the interlayer coupling involves the 12 nearest neighbours for which the Fe-S-Fe bond angle is closest to 180° (the optimal angle for superexchange). In other words the central Fe atom in Fig. 3(a) interacts most strongly with the 12 Fe atoms defining the hexagonal upper and lower faces of the unit cell (for which the bond angle = 132°) and much more weakly with atoms directly above and below or in the same layer (with bond angles 71° and 90° respectively).

Composition independence of the Néel temperature and Curie constants (Lotgering, 1956) indicate that exchange interactions in the range FeS-Fe_7S_8 are approximately constant.

Above the Néel temperature, T_N, pyrrhotites obey the Curie-Weiss Law $\chi = C/(T-\theta)$, where χ is susceptibility, C is the Curie constant and θ the Weiss temperature. Molecular field constants are related to T_N, θ, C and $\chi(T_N)$ (Morrish, 1965, pp. 447-453).

Denote the intralayer molecular field constant by $N_1 = N_{ii}$ and the interlayer constant by $N_2 = N_{AB}$ (defined such that the molecular field acting on an atom in sublattice A is $N_{ii}M_A + N_{AB}M_B = N_1M_A + N_2M_B$ and similarly for sublattice B).

Then,

$$N_1 = (\theta + T_N)/C \qquad (1)$$

$$N_2 = (\theta - T_N)/C \qquad (2)$$

$$N_2 = 1/\chi\ (T_N) \qquad (3)$$

Experimental determinations of T_N, θ, C and $\chi(T_N)$ for FeS and Fe_7S_8 are listed in Table 1.

For FeS the mean values are T_N = 601K, θ = -978K, C_{mole} = 3.5 ($\therefore$ C = 0.183GK/oe) and $\chi(T_N) = 25 \times 10^{-6}$ Gcm^3/g oe.

From (1) and (2) we get N_1 = -108 (per mole) = -2060 (per cm^3), and N_2 = -451 (per mole) = -8630 (per cm^3). A consistency check is provided by (3) which gives

N_2 = -8700 (per cm^3), in good agreement with (2). The negative signs imply both interactions are antiferromagnetic with interlayer coupling dominating.

The Curie constant is given by

$$C = Ng^2\mu_B{}^2S(S + 1)/3k \qquad (4)$$

Where N is the number of Fe atoms per cm^3 (or per mole if we are considering C_{mole}), g is the gyromagnetic ratio, μ_B is the Bohr magneton, S is the spin quantum number and k is Boltzmann's constant.

Scott and Meyer (1961) measured the gyromagnetic ratio of monoclinic pyrrhotite using the Einstein-de Haas method. They found g = 1.9 ± 0.3, consistent with complete quenching of orbital angular momentum (for which case the spin-only value g=2 applies). Taking N = 3.1 x 10^{22}, μ_B = 9.27 x 10^{-21} erg/G, k = 1.38 x 10^{-16} erg/K gives S = 2.2 for FeS, which is slightly more than the value for an isolated Fe^{2+} ion (S = 2) suggesting there is some orbital contribution to the magnetic moment in FeS.

Exchange integrals may also be estimated from paramagnetic susceptibility data. Denote the intralayer exchange integral by J_1, with z_1 neighbours, and the interlayer exchange integral by J_2, with z_2 neighbours. Smart (1963) gives the following expressions for layer lattices with type I ordering (as in pyrrhotite):

$$z_1J_1 - z_2J_2 = 3kT_N/2S(S + 1) \qquad (5)$$

$$z_1J_1 + z_2J_2 = 3k\theta/2S(S+1) \quad (6)$$

$$-2z_2J_2 = 3kC/2\ \chi(T_N)S(S+1) \quad (7)$$

from which we obtain $z_1J_1/k = -40K$, $z_2J_2/k = -168K$ and $z_2J_2/k = -170K$, taking $S = 2.2$ and using (5), (6) and (7) respectively. Assuming $z_1 = 6$ and $z_2 = 12$ gives $J_1/k = -7K$ and $J_2/k = -14K$.

In the absence of anisotropy energy the susceptibility of antiferromagnets perpendicular to the spin direction is temperature independent. Thus the measurements by Horwood et al. (1976) of basal plane susceptibility of nearly stoichiometric FeS allow estimation of the change in z_2J_2 at the α-transition, as the spins are along the c-axis up to T_S ($>T_\alpha$). For this sample $C_{mole} = 3.74$, which corresponds to $S = 2.3$. The basal plane susceptibility increases from 15×10^{-6} Gcm^3/goe to 25×10^{-6} Gcm^3/goe at T_α, which from (7) indicates a decrease in $z_2|J_2|/k$ from 280K to 168K.

Marusak (1979) has estimated z_2J_2/k for Fe_7S_8 from measurements of the pressure dependence of saturation magnetisation, Néel temperature and volume, neglecting J_1. He finds $z_2J_2/k = -210K$, in reasonable agreement with the value obtained above for FeS.

A completely independent estimate of z_2J_2/k has also been obtained by Marusak (1979), based on least-squares fitting of Mössbauer data to a crystal field model including exchange interaction. It can be seen from Fig. 1 that

there are 4 inequivalent Fe sites in Fe_7S_8: (1) in filled layers with a vacancy directly above or below, (2) in a vacancy layer with 2 nearest neighbour vacancies, (3) in a filled layer with Fe atoms above and below and (4) in a vacancy layer with 2 nearest neighbour and 2 next-nearest neighbour vacancies. Let the exchange integrals (equivalent to J_2) in the a and c directions (parallel and perpendicular to the spins respectively) be J_a and J_c. It is found that sites 2 and 4 are more or less isotropic whereas sites 1 and 3 are strongly anisotropic (Table 2).

Marusak (1979) finds $S \simeq 1$ for Fe_7S_8, which is significantly lower than the value S = 2 applicable to high spin ferrous iron, and attributes the low effective moment to mixing of spin components due to obliquity of the hyperfine field to the axis of axial distortion. This value of S is consistent with the observed saturation magnetisation of Fe_7S_8 ($\sim$20 emu/g) which corresponds to $2.33\mu_B$ per Fe atom, or $S = 2.33/g \simeq 1.2$. The decrease in effective moment with increasing iron deficiency is probably a result of the increasing covalency from FeS to Fe_7S_8 found by Gosselin et al. (1976). The various ionic models invoked to explain the low spontaneous magnetisation of Fe_7S_8 appear to be ruled out by Mössbauer spectroscopy which detects no ferric iron.

Application of (5) - (7) to the data given in Table 2 for Fe_7S_8 reveals discrepancies. The values obtained are: $z_1J_1/k = -278K$, $z_2J_2/k = -614K$ and $z_2J_2 = -89K$ respectively (using S = 1.2). The relations

(5) - (7) are based on molecular field theory which is not really satisfactory for estimation of exchange interactions in ferrimagnetic substances (Smart, 1963). The value obtained from (7) is probably a gross underestimate due to contamination of the sample by traces of magnetite. In addition anisotropy energy has been neglected.

Wanic (1964) studied inelastic neutron scattering from a natural crystal of $Fe_{0.88}S$ (monoclinic pyrrhotite). From the magnon dispersion relations for the acoustic branch and from spin-wave theory he obtained $J_2 = -1.1$ meV or $J_2/k = -13K$ by taking $S = 2$ and assuming $J_2 = J_2'$, where J_2' is the exchange integral between Fe atoms directly above one another. However J_2' should be much less than J_2 due to the Fe-S-Fe bond angles involved. In this case the expression given by Wanic reduces to:

$$-4\pi J_2 \, a \, (72 S_A S_B)^{\frac{1}{2}} = 810 \text{ meV.AU} \qquad (8)$$

Taking $a = 3.44$ AU, $S_A = 1.2$, $S_B = 1.2 \times 7/8$ gives $J_2 = -2.0$ meV, or $J_2/k = -23K$.

Knowledge of spin-wave dispersion in pyrrhotite also allows calculation of the frequency factor for thermal activation in multidomain pyrrhotite. The domain wall thickness in pyrrhotite is calculated to be approximately 40AU. A spin-wave with half-wave length equal to the wall thickness therefore has wave-vector $q = 2\pi/80$ $AU^{-1} \simeq 80$ mAU^{-1}. This corresponds to a spin-wave energy of ~50 meV. Equating hf to this value gives $f \simeq 10^{13}$ Hz, at the upper limit of values given in the literature for ferro- and ferrimagnetic materials.

Krasnicki et al. (1964) determined the temperature dependence of spin fluctuation scattering of neutrons from pyrrhotite. Exchange interactions were found to vary little with temperature.

Unidirectional properties due to exchange anisotropy have been studied in sulphided iron films (Greiner, 1966). The anisotropy arises from exchange coupling between ferromagnetic Fe and antiferromagnetic FeS.

In summary, exchange interactions in $Fe_{1-x}S$ are characterised by relatively strong antiferromagnetic interlayer coupling with $J_2/k \simeq -20K$ and intralayer coupling which is also antiferromagnetic but about half the magnitude of J_2 ($J_1/k \simeq -10K$). Interlayer coupling probably involves ~12 neighbours whereas intralayer coupling involves ~6 neighbours (depending slightly on composition).

3. Magnetocrystalline anisotropy and magnetostriction in pyrrhotites

Referring to the crystal structure of Fe_7S_8 depicted in Fig. 1 , let us define polar angle θ measured from the orthorhombic c-axis and an azimuthal angle ϕ, measured from the easy magnetic direction within the basal plane. Then the magnetocrystalline anisotropy energy can be expressed as:

$$E_K = -K_0|\cos\theta| + K_1\sin^2\phi\sin^2\theta + K_2\sin^4\phi\sin^4\theta + K_3\cos^2\theta + K_4\cos^4\theta + K_5\sin^2\phi\cos^2\theta\sin^2\theta + \ldots \quad (9)$$

where the conventional anisotropy constants $K_1,\ldots,K_5$ have

their usual meanings. The $K_0|\cos\theta|$ term is required to fit magnetisation curve data at low temperatures (Hirone et al., 1964) and has been explained by a theoretical model of anisotropy in pyrrhotite (Adachi and Sato, 1968).

Experimental determinations of anisotropy constants in 4C Fe_7S_8 are summarised in Table 3. Two main methods have been employed: high-field magnetisation (J-H) curves and high-field torquemeter measurements. There is substantial variation in the estimates of anisotropy constants from different studies, but a number of conclusions can nevertheless be drawn.

At room temperature the magnetic moment of ferrimagnetic pyrrhotite is essentially confined to the basal plane by strong magnetocrystalline anisotropy, an applied field of ~70 koe being required to align the moment with the c-axis. For this reason the estimates of K_3 and K_4 obtained in fields of $\leq$ 20 koe by Bin and Pauthenet (1963) are less reliable than those from studies which used higher fields.

A reasonable estimate of K_3 is 3×10^6 erg/cm^3, with K_4 serving as a correction factor. K_0 is also small at room temperature.

Anisotropy within the basal plane is much smaller, but nevertheless substantial. The preferred value of K_1 is ~3×10^5 erg/cm^3, with K_2 significantly less than K_1.

Below room temperature the anisotropy constants change significantly and the spontaneous magnetisation gradually departs from the basal plane (Bin and Pauthenet, 1963;

Besnus, 1966) until approximately 20^{o} out of the basal plane ($\theta \approx 70^{o}$). Bin and Pauthenet (1963) did not consider the K_o term and related the rotation of easy direction to a change in sign of K_3 at 200K, at which temperature K_4 passes through a maximum, followed by monotonic decreases in K_3 (<0) and K_4. The stable angle of the magnetic moment is then $\theta_0 = \cos^{-1}(-K_3/2K_4)^{\frac{1}{2}}$ for $K_3<0$ and $K_3 + 2K_4 > 0$. On the other hand if the anisotropy is dominated by K_0 and K_3, θ_0 is given by $\cos^{-1}(K_0/2K_3)$.

Torque measurements in the basal plane (Mikami et al., 1959; Hirone et al., 1962) reveal a triad domain structure in which easy directions of magnetisation are related by 120^{o} rotations about the c-axis. The proportions of each twin member are not necessarily equal.

The triad domain structure is related to crystallographic twinning, but the literature is ambiguous on the crystallographic orientation of the easy magnetic direction within each twin. Mikami et al. (1959) found that the easy directions coincided with orthorhombic a-axes above $-80^{o}C$, but lay along the b-axes of the twin members below that temperature. This suggests the possibility of low-temperature cleaning of multidomain pyrrhotite, analogous to the technique used for magnetite.*

The change of easy direction is presumably associated with a change in sign of K_1 at $-80^{o}C$. However no isotropic point nor anomalous behaviour of basal plane anisotropy constants was observed below room temperature by either Bin

* Throughout this report it is assumed that the easy direction is in fact the a-axis, but this does not materially affect any of the subsequent discussion.

and Pauthenet (1963) or Besnus (1966).

The work of Besnus (1966) reveals difficulties with the concept of magnetocrystalline anisotropy as defined by eq. 9. Consistent values for K_0, K_3 and K_4 cannot be found which satisfy all the experimental data (the spontaneous magnetisation component, the susceptibility and the coercive force, all measured along the c-axis) at low temperatures. However it is possible that the anomalously low coercive force measured along the c-axis may be a result of domain structure. Movement of domain walls in response to fields applied along c would significantly lower the critical fields from the "single domain" value assumed by Besnus.

It is found that the c-axis remains a very hard axis of magnetisation even at 285°C, quite close to the Néel point. This suggests that K_3 cannot be regarded as a conventional magnetocrystalline anisotropy constant which would be expected to tend rapidly to zero at the Néel temperature. K_1 and K_2, on the other hand, do tend to zero at T_N as expected and can be interpreted as ordinary magnetocrystalline anisotropy constants.

The virtual temperature independence of susceptibility along the c-axis is analogous to that of the perpendicular susceptibility of an antiferromagnet.

The analogy with antiferromagnetic materials is supported by the high degree of compensation of the sublattices in pyrrhotite.

Besnus (1966) and Besnus et al. (1968) proposed a molecular field model incorporating sublattice anisotropy constants to explain the experimental data. The two sublattices have magnetisations $\underset{\sim}{J}$ and $\underset{\sim}{J}'$ making angles θ and θ' respectively with the c-axis. The equilibrium states in an applied Field $\underset{\sim}{H}$ are found by minimising the energy expression

$$E = N_w JJ' \cos(\theta-\theta') + K\sin^2\theta + K'\sin^2\theta' - \underset{\sim}{H}.(\underset{\sim}{J}+\underset{\sim}{J}') \qquad (10)$$

where N_w is the molecular field coefficient and K and K' are sublattice anisotropy constants.

The susceptibility along c is approximately $1/N_w$ and is almost temperature independent. N_w is found to be $\sim 2\times10^3$, of the same order of magnitude as the value deduced from the Curie-Weiss Law. At room temperature K and K' are deduced to be $\sim -10^7$ erg/cm^3 , but below room temperature K changes sign leading to a non-colinear (canted) configuration of the sublattices and the appearance of a spontaneous magnetisation component along the c-axis.

The weak anisotropy of FeS above the Néel temperature has been measured by Murakami (1959) and has been interpreted to arise from the anisotropy of the crystalline field. The results indicate that above T_N there is a weak preferred orientation of spins parallel to the c-axis, indicating the anisotropy constant changes its sign at T_N.

The thermal variation of the magnetostriction of pyrrhotite in an applied field of 1880 oe has been determined by Belov and Zalesskii (1958). The sample used after heating to 350^{o}C had a saturation magnetisation of 16 emu/g.

The magnetostriction constant λ at room temperature is positive and small ($\lambda = 1.0 \times 10^{-5}$) and decreases with increasing temperature, approximately as J_s. The absence of stress patterns in domain structures of polished pyrrhotite grains also indicates that the magnetostriction of pyrrhotite is much smaller than that of titanomagnetites (Soffel, 1977). The forced volume magnetostriction of Fe_7S_8 has been determined by Marusak (1979) to be 1.4×10^{-9} oe^{-1} at room temperature.

4. Thermomagnetics of pyrrhotites

Following studies of thermomagnetic properties of natural samples by Hayase et al. (1963), Takeno (1966) and Schwarz (1973), natural pyrrhotites can be classified into 4 categories on the basis of their high-field thermomagnetic curves:

(i) Samples exhibiting low susceptibility ($<10^{-3}$G/oe) across the temperature range 0 - 350°C and zero spontaneous magnetisation. For these samples $x<0.08$, corresponding to 2C + 6C pyrrhotite assemblages.

(ii) Samples exhibiting zero spontaneous magnetisation at room temperature but which are ferrimagnetic in a relatively narrow temperature range about ~200°C. The high-field (J-T) thermomagnetic curves are characterised by a pronounced peak at the so-called γ-transition and are referred to as "peak-type" curves. The room temperature susceptibility is in the range 2-6 $\times 10^{-3}$ G/oe and the apparent saturation magnetisation in ~10koe at T_γ is

~4-7 emu/g. These samples have $0.09 \leq x \leq 0.10$, corresponding to intermediate pyrrhotites in the range $Fe_{10}S_{11}$ - Fe_9S_{10}. The γ-transition is most pronounced for 5C pyrrhotite (Fe_9S_{10}).

(iii) Samples which are ferrimagnetic at room temperature with J_s ~ 16-21 emu/g, exhibiting a normal "Weiss-type" J-T curve, with steady decrease of magnetisation up to an apparent Curie temperature of ~320°C. These samples are monoclinic 4C pyrrhotites with $x > 0.12$.

(iv) Samples with properties intermediate between types (ii) and (iii). The samples are mixtures of monoclinic and peak-type intermediate pyrrhotites and the thermomagnetic curves are Weiss-type with superimposed peaks.

This classification demonstrates the potential of qualitative analysis of pyrrhotites by thermomagnetic measurements. Furthermore, a large body of experimental data on thermomagnetics of synthetic pyrrhotites is available in the literature which suggests the possibility of detailed quantitative analysis of natural pyrrhotites, given recent advances in our knowledge of the mineralogy, crystallography and phase relations of pyrrhotites. Synthetic preparations of $Fe_{1-x}S$ often represent metastable phases which are rare or unknown in nature and this fact must be borne in mind before thermomagnetic curves of natural pyrrhotites can be reliably interpreted.

Thermomagnetic curves of $Fe_{1-x}S$ reflect a number of

crystallographic and magnetic transitions, which in general are composition dependent. The thermomagnetic expression of each of these transitions will be discussed in turn.

α-transition - In near stoichiometric FeS the transition from the 2C (low-troilite) structure to the 1C structure is accompanied by a marked increase in susceptibility (by about 70% in FeS) due to a decrease in strength of the exchange interaction. Thermal hysteresis at this transition is often quite pronounced and probably reflects kinetics of the low-troilite to transitional troilite transformation.

With increasing x, T_α decreases and the magnetic expression of the transition becomes less prominent. A slight knick in the J-T curves corresponding to T_α can be traced up to $x \simeq 0.091$ ($Fe_{10}S_{11}$), although the crystallographic significance of the magnetic transition is clearly not equivalent to that at $x \simeq 0$.

In troilite T_α is also a ferroelectric Curie temperature (the 2C structure is ferroelectric and 1C is paraelectric) as shown by Van den Berg et al. (1969).

Morin transition - the strongly composition dependent spin-flip transition appears as a knick in J-T curves. For $x>0.03$, T_s is below room temperature and decreases rapidly with increasing x. This transition can be conceptually extended to $x=0.125$ (Fe_7S_8) which exhibits a very gradual partial spin-flip with θ decreasing from 90° to 70° between 200K and 4K.

γ-transition - this represents a crystallographic

transition involving changes in vacancy ordering schemes, accompanied by the appearance of ferrimagnetism. T_γ is defined as the temperature at which the saturation magnetisation peaks. The lower bound of the γ-region is called the Haraldsen or anti-Curie point, T_H, and the upper limit is generally referred to as the Curie temperature, T_C. T_H marks an antiferromagnetic-ferrimagnetic transition and T_C represents a ferrimagnetic-antiferromagnetic transition. Thus T_C is not a true Curie temperature as the loss of spontaneous magnetisation does not indicate spin disordering with the onset of paramagnetism. The apparent Curie temperature in fact corresponds to a crystallographic transformation - the disordering of vacancies to form the antiferromagnetic 1C structure - and occurs significantly below the spin disordering temperature (the Néel point) for all compositions except ~Fe_7S_8.

The γ-transition first appears on thermomagnetic curves as a slight kink at ~130°C for $x \simeq 0.05$ which, as x increases, develops into a cusp and then a spectacular Λ- shaped peak for $x \simeq 0.1$ at progressively higher temperatures (e.g. $T_\gamma \simeq 215^\circ C$ for Fe_9S_{10}). The γ-transition is not reversible on cooling unless the cooling is very slow. This is because vacancy diffusion in $Fe_{1-x}S$ occurs over a time-scale comparable to that of thermomagnetic runs (minutes to hours) at these temperatures. Magnetic methods are therefore a convenient means of studying vacancy diffusion in intermediate pyrrhotites (Marusak, 1979; Townsend et al., 1979; Bennett and Graham, 1981).

Although T_H, T_γ and T_C vary systematically with composition there are some discrepancies in values reported in the

literature, probably largely reflecting different rates of temperature change. Kinetic difficulties are indicated by thermal hysteresis at T_H and, to a lesser extent, at T_C. Therefore for quantitative analysis thermomagnetic equipment should be calibrated against known pyrrhotite composition for standardised heating and cooling rates.

β-transition - this is the Néel point of $Fe_{1-x}S$ and unlike the other transitions is independent of composition, occurring at approximately 325°C for $0 \leq x \leq 0.125$ (FeS - Fe_7S_8).

For $x<0.125$, T_β is observed as a slight cusp in thermomagnetic curves, as expected for antiferromagnetic substances for which susceptibility is a maximum at T_N. The β-transition is not clearly identifiable in thermomagnetic curves of monoclinic pyrrhotite because of the close proximity of the apparent Curie temperature.

Typical high-field thermomagnetic curves of FeS, Fe_9S_{10} and Fe_7S_8 are illustrated in Fig. 4 , Fig. 5(a) and Fig. 5(b) respectively. The composition dependence of the transition temperatures, volume susceptibility and saturation magnetisation is summarised in Table 4.

Thermomagnetics of intermediate pyrrhotite can be interpreted in terms of the phase diagram (Fig. 6). T_H represents the temperature at which substantial variation of N in the NC superstructures is initiated. The data of Nakazawa and Morimoto (1971) and Sugaki et al. (1971) indicate that N decreases (apparently continuously) from 5.0 - 6.0 to 3.0 - 4.0 between ~100°C and ~200°C. The change in N presumably reflects the presence of varying

proportions of domains possessing relatively ordered structures, stacked along the c-axis with varying degrees of long range order. Domains with N = 4.0 and N = 3.0 are ferrimagnetic and their presence significantly enhances the susceptibility, but in the absence of long range order the material as a whole does not possess spontaneous magnetisation, i.e. the substance is still antiferromagnetic in bulk.

T_γ corresponds to the transformation to NA pyrrhotite with full development of ferrimagnetism and T_C represents the transformation to the antiferromagnetic 1C or MC (M non-integral) structures. The phase diagram accounts for the very weak γ-anonaly in 6C pyrrhotite ($Fe_{11}S_{12}$), which transforms directly from NC to 1C, as opposed to 11C ($Fe_{10}S_{11}$) or 5C (Fe_9S_{10}) pyrrhotites, which exhibit pronounced peaks in thermomagnetic curves associated with the NC-NA transformation.

Marusak and Mulay (1979) suggest the γ-transition in Fe_9S_{10} represents a gradual transformation from 5C to 4C superstructure, but this is based on X-ray diffraction of Fe_9S_{10} quenched from T_γ. The observed 4C superstructure probably results from alternative metastable behaviour during quenching.

For monoclinic pyrrhotite, on the other hand, the phase diagram indicates non-integral pyrrhotites + pyrite as the stable assemblages above ~250°C. However exsolution of pyrite from monoclinic pyrrhotite requires months at ~300°C, so the phase relations proper are not relevant to thermomagnetic

behaviour of monoclinic pyrrhotite.

The evidence indicates a transformation from 4C to 1C pyrrhotite (Corlett, 1964; Taylor, 1970; Nakazawa and Morimoto, 1971; Sugaki et al., 1977) at a rate which depends on temperature (in minutes at 330°C) or, equivalently, at a temperature, T_V, which depends on heating rate (~250° for very slow heating, up to ~340°C for rapid heating). The transformation is reversible on slow cooling, but on quenching a 3C superstructure is formed (NA type or 2A,3C type).

Thermomagnetic curves of monoclinic pyrrhotite reported in the literature give apparent Curie temperatures in the range 300-325°C, presumably reflecting different heating rates, and are generally very reversible, although thermal hysteresis at T_C is sometimes observed (e.g. Besnus, 1966). The upper limit to T_C is, of course, the Néel point at 325°C, so $T_C = T_V$ or T_β , whichever is the lesser.

Although high-field thermomagnetic (J_s-T) curves are abundant in the literature, low-field (k-T) curves of pyrrhotites do not appear to have been studied. This is surprising in view of the essentially complementary information provided by J_s-T and k-T curves. Whereas saturation magnetisation is an intrinsic property of a magnetic material, magnetic susceptibility is structure dependent. Both types of curve allow determination of magnetic transition temperatures, yielding information on composition, but J_s-T curves are more suited to quantitative analysis of magnetic phases, while k-T measurements elucidate domain

structure, grain size, blocking temperatures and other data important to rock magnetic and palaeomagnetic studies.

Typical k-T curves of monoclinic, peak-type intermediate and mixed-type pyrrhotites are illustrated in Fig. 7. The susceptibility of powdered samples in a quartz tube was measured in ~1 oe using a transformer bridge with a bifilar-wound furnace surrounded by a water jacket. Temperature was measured using a platinum resistance thermometer inserted into the sample. The quartz tube could be evacuated or filled with nitrogen.

Monoclinic pyrrhotites invariably display a rise in susceptibility of about 30% between -200°C and 20°C. This feature, which has not been reported before, may reflect gradual departure of the spontaneous magnetisation from the basal plane at low temperatures with consequent perturbation of domain structure. The J_s-T curve of these pyrrhotites is Weiss-type between -200°C and T_c, but is anomalous at lower temperatures, with J_s passing through a broad maximum at ~50K (Besnus and Meyer, 1964).

A Hopkinson peak, representing unblocking of grains and transition to the superparamagnetic state, is exhibited by all monoclinic pyrrhotite samples tested between, typically, ~200°C and a point immediately below the apparent Curie temperature at ~325°C. The extremely rapid descent of the curves at T_c, the negligible thermal hysteresis and the relatively high value of T_c suggest that at the heating and cooling rates employed (~10°C/minute) T_c represents the

magnetic β-transition (Néel point) rather than the vacancy disordering temperature T_V. Interpretation of the peak below T_C as a Hopkinson peak rather than the effect of chemical or structural change is confirmed by reversibility of the curves.

At higher temperatures chemical changes are common, particularly if the heating takes place in air. Magnetite is often produced, rendering the curves highly irreversible. Some of the changes that can occur and their magnetic effects are discussed by Bennett and Graham (1980).

The k-T curves for peak-type pyrrhotites, as expected, are highly irreversible with large increases of susceptibility after heating to 350°C. These pyrrhotites seem to be more prone to oxidation than monoclinic pyrrhotite and magnetite is often produced along with conversion of intermediate to monoclinic pyrrhotite. These remarks also apply to the peak-type component of mixed-type pyrrhotites.

5. Self-reversal of remanent magnetisation

Palaeomagnetic results from some pyrrhotite-bearing rocks (e.g. Almond et al., 1956; Everitt, 1962; Robertson, 1963) suggest the intriguing possibility that the rocks bear self-reversed remanence (remanence direction antiparallel to the ambient field at the time of acquisition). This possibility is supported by laboratory demonstration of full self-reversal of thermoremanence in a pyrrhotite-bearing

shale by Everitt (1962) and partial self-reversal in a number of natural pyrrhotite samples by Bhimasankaram and Lewis (1966).

Self-reversal has important implications for palaeomagnetism and magnetostratigraphy, as when the magnetic mineralogy is dominated by pyrrhotite, remanence polarity cannot be confidently interpreted in terms of palaeofield polarity in the absence of definitive field evidence.

The self-reversal phenomena observed by Everitt (1962) and Bhimasankaram and Lewis (1966) are quite different in detail and their results will be summarised in turn.

The shale studied by Everitt contained a narrow band within which the natural remanent magnetisation (NRM) was reversed with respect to the surrounding rock and which exhibited anomalous thermomagnetic properties.

On continuous thermal demagnetisation in zero field the anomalous material reversed its NRM at ~150°C, the reversed magnetisation peaked at ~250°C and then gradually reduced to zero at ~350°C.

High-field thermomagnetic measurements indicate that the anomalous magnetic material alters on heat treatment at ~310°C to a Weiss-type pyrrhotite. Everitt hypothesises that the original material is an anomalous type of pyrrhotite which he calls "A", which alters to material "B". Examination of the J_s-T curve for material A, in the light of more recent knowledge, shows that A is mixed-type pyrrhotite with $T_H \simeq 150^{\circ}C$ and T_γ between 200°C and 250°C.

The properties of the anomalous material were very sensitive to the temperature of heat treatment. Heating between 313°C and 320°C caused saturation remanence to self-reverse, whereas between 300°C and 313°C only partial self-reversal was observed.

The evidence suggests the self-reversal is due to magnetostatic interaction between the parent and altered material (mixed-type and Weiss-type pyrrhotites respectively. The strength of the interaction field is ~10 oe, which is far too small to represent exchange interaction between phases. The evidence is insufficient to determine the precise crystallographic and chemical nature of the transformation of the parent material.

Bhimasankaram and Lewis worked with massive pyrrhotite samples. These authors could not explain the initial J_s-T curves of their samples, but it is clear that the initial material is mixed-type pyrrhotite which oxidises above ~400°C on initial heating, forming variable quantities of magnetite (T_C = 580°C) and converting the pyrrhotite to Weiss-type. The chemical change involves removal of iron from the intermediate pyrrhotite initially present, transforming it to the more iron-deficient monoclinic pyrrhotite. After heating to ~600°C the material has a fully reversible J_s-T curve with two Curie temperatures (320°C and 580°C).

When such a sample is cooled from 600°C to 350°C in a field of 0.5 oe, the material acquires a normal thermoremanence. If the field is switched off during subsequent cooling the

remanence self-reverses at ~300°C, whereas if the field is maintained throughout cooling the room-temperature remanence is normal.

Detailed experiments show that the partial self-reversal is due to interaction between the phases with the high and low Curie temperatures. The interaction field is ~0.1 oe and is clearly magnetostatic in origin.

AF demagnetisation preferentially removes the reversed component and chemical demagnetisation in concentrated HCl enhances it. These results are consistent with identification of the normally magnetised phase as magnetite lamellae within a much larger bulk of monoclinic pyrrhotite. Thin lamellae of magnetite within natural pyrrhotite have been described by Bennett et al. (1972a, 1972b). Microscopic identification, or even detection, of these lamellae is usually very difficult. Although Bennett et al. (1972a) attribute self-reversal in pyrrhotite to submicroscopic lamellae of smythite within pyrrhotite grains, thermomagnetic curves indicate that magnetite is commonly produced during heating in air or vacuum of natural pyrrhotites above 400°C, and is almost invariably initially present in small quantities in synthetic and natural samples (e.g. Lotgering, 1956; Besnus, 1966; Bhimasankaram and Lewis, 1966; Bennett and Graham, 1980).

Given that at least two distinct types of self-reversal phenomena can be demonstrated in the laboratory, a number of possible natural processes can be envisaged which could

produce irreproducible self-reversed remanence in pyrrhotite-bearing rocks. Néel (1955) has reviewed possible self-reversal mechanisms, evidence of which may easily be obliterated by subsequent geological events.

6. References

Adachi, K. and Sato, K., 1968. Origin of magnetic anisotropy energy of Fe_7S_8 and Fe_7Se_8. J. Appl. Phys., 39: 1343-1344.

Almond, M., Clegg, J.A. and Jaeger, J.C., 1956. Remanent magnetism of some dolerites, basalts and volcanic tuffs from Tasmania. Phil. Mag., 1: 771-782.

Andresen, A.F. and Torbo, P., 1967. Phase transitions in Fe_xS (x=0.90-1.00) studied by neutron diffraction. Acta Chem. Scand., 21: 2841-2848.

Belov, K.P. and Zalesskii, 1958. Thermal expansion and magnetostriction of pyrrhotite. Soviet Physics-Crystallography, 3: 390-392.

Bennett, C.E.G., Graham, J. and Thornber, M.R., 1972a. New observations on natural pyrrhotites. Part I. Mineragraphic techniques. Am. Mineral., 57: 445-462.

Bennett, C.E.G., Graham, J., Parks, T.C. and Thornber, M.R. 1972b. New observations on natural pyrrhotites. Part II. Lamellar magnetite in monoclinic pyrrhotite. Am. Mineral., 57: 1876-1880.

Bennett, C.E.G. and Graham, J., 1980. New observations on natural pyrrhotites. Part III. Thermomagnetic experiments. Am. Mineral, 65: 800-807.

Bennett, C.E.G. and Graham, J., 1981. New observations on natural pyrrhotites: magnetic transition in hexagonal pyrrhotite. Am. Mineral., 66: 1254-1257.

Besnus, M.J., 1966. Propriétés magnétiques de la pyrrhotine naturelle. Thèse, Université de Strasbourg.

Besnus, M.J. and Meyer, A.J.P., 1964. Nouvelles données experimentals sur le magnétisme de la pyrrhotine naturelle. Proceedings of the International Conference on Magnetism, Nottingham, Sept. 1964, pp. 507-511.

Besnus, M.J., Munschy, G. and Meyer, A.J.P., 1968. Sublattice rotations in ferrimagnets: the case of pyrrhotite. J. Appl. Phys., 39: 903-904.

Bhimasankaram, V.L.S. and Lewis, M., 1966. Magnetic reversal phenomena in pyrrhotite. Geophys. J. R. astron. Soc., 11: 485-497.

Bin, M. and Pauthenet, R., 1963. Magnetic anisotropy in pyrrhotite. J. Appl. Phys., 34: 1161-1162.

Chikazumi, S. and Charap, S.H., 1978. Physics of Magnetism. Krieger, Huntington (N.Y.), 544pp.

Corlett, M., 1964. Mineralogy of pyrrhotite. Ph.D. Thesis Univ. of Chicago.

Everitt, C.W.F., 1962. Self-reversal of magnetization in a shale containing pyrrhotite. Philos. Mag., 7: 831-842.

Gosselin, J.R., Townsend, M.G., Tremblay, R.J. and Webster, A.H., 1976. Mössbauer effect in single-crystal $Fe_{1-x}S$. J. Solid State Chem., 17: 43-48.

Greiner, J.H., 1966. Exchange anistropy properties in sulfided iron films. J. Appl. Phys., 37: 1474-1475.

Haraldsen, H., 1941a. Über die hochtemperaturumwandlungen der eisen (II) - sulfidmischkristalle. Z. anorg. allg. Chem., 246: 195-226.

Haraldsen, H., 1941b. Über die eisen (II) - sulfidmisch-kristalle. Z. anorg. allg. Chem., 246: 169-194.

Hayase, K., Otsuka, R. and Mariko, T., 1963. On the magnetic properties of natural pyrrhotites. Mineral. J., 4: 41-56.

Hihara, T., 1960. Magnetic and electrical properties of iron sulfide single crystals. J. Sci. Hiroshima Univ., Ser. A., 24: 31-53.

Hirahara, E. and Murakami, 1958. Magnetic and electrical anisotropies of iron sulfide single crystals. J. Phys. Chem. Solids, 7: 281-289.

Hirone, T., Adachi, K., Yamada, M., Chiba, S. and Tazawa, S., 1962. The magnetic anisotropy of pyrrhotite and iron selenide. J. Phys. Soc. Japan, 17: 257-260.

Hirone, T., Maeda, S., Chiba, S. and Tsuya. N., 1954. Thermal analysis of iron sulfides at the temperature range of the β-transformation. J. Phys. Soc. Japan, 9: 500-502.

Hirone, T., Sato, K. and Yamada, M., 1964. Magneto-crystalline anisotropy of a pyrrhotite crystal (Fe_7S_8). Proceedings of the International Conference on Magnetism, Nottingham, Sept. 1964, pp.505-506.

Horita, H. and Hirahara, E., 1971. Mössbauer studies of single crystal iron sulfide. Sci. Rpts Tohoku Univ., 54: 127-169.

Horwood, J.L., Townsend, M.G. and Webster, A.H., 1976. Magnetic susceptibility of single-crystal $Fe_{1-x}S$. J. Solid State Chem., 17: 35-42.

Krasnicki, Sz., Wanic, A., Dimitrijevic, Z., Maglic, R., Markovic, V. and Todorovic, J., 1964. Temperature dependence of spin fluctuation scattering of neutrons on pyrrhotite. J. de Physique, 25: 634-641.

Lotgering, F.K., 1956. On the ferrimagnetism of some sulphides and oxides. Philips Res. Repts, 11: 190-217.

Marusak, L.A., 1979. Moessbauer and magnetic studies of some iron sulfides. Ph.D. thesis, Pennsylvania State University.

Marusak, L.A. and Mulay, L.N., 1979. Mössbauer and magnetic study of the antiferro to ferrimagnetic phase transition in Fe_9S_{10} and the magnetokinetics of the diffusion of iron atoms during the transition. J. Appl. Phys., 50: 1865-1867.

Mikami, I., Hirone, T., Watanabe, H., Maeda, S. and Adachi, K., 1959. On the magnetic anistropy of a pyrrhotite crystal. J. Phys. Soc. Japan, 14: 1568-1572.

Morrish, A.H., 1965. The Physical Principles of Magnetism. Wiley, New York, 680pp.

Murakami, M., 1959. Anisotropy energy in the paramagnetic region of iron sulfide. Sci. Rpts. Tohoku Univ., 43: 62-66.

Nakazawa, H. and Morimoto, N., 1971. Phase relations and superstructures of pyrrhotite, $Fe_{1-x}S$. Mat. Res. Bull., 6: 345-358.

Néel, L., 1953. Some new results on antiferromagnetism and ferromagnetism. Rev. Mod. Phys., 25: 58-63.

Néel, L., 1955. Some theoretical aspects of rock magnetism. Adv. Phys., 4: 191-243.

Perthel, R., 1960. Über den ferrimagnetismus nichtstöchiometrischer eisensulfide. Ann. Physik, 5: 273-295.

Power, L.F. and Fine, H.A., 1976. The iron-sulphur system. Part I. The structure and physical properties of the compounds of the low-temperature phase fields. Minerals Sci. Engng., 8: 106-128.

Robertson, W.A., 1963. Paleomagnetism of some Mesozoic intrusives and tuffs from Eastern Australia. J. Geophys. Res., 68: 2299-2312.

Sato, K., 1966. Magnetizing process of pyrrhotite crystal in high magnetic field. J. Phys. Soc. Japan, 21: 733-737.

Sato, K., Yamada, M. and Hirone, T., 1964. Magnetocrystalline anisotropy of pyrrhotite. J. Phys. Soc. Japan, 19: 1592-1595.

Schwarz, E.J., 1973. Magnetic characteristics of massive sulphide ore bodies near Sudbury, Canada. Can. J. Earth Sci., 10: 1735-1743.

Schwarz, E.J. and Vaughn, D.J., 1972. Magnetic phase relations of pyrrhotite. J. Geomagn. Geoelectr., 24: 441-458.

Scott, G.G. and Meyer, A.J.P., 1961. Gyromagnetic ratio of pyrrhotite. Phys. Rev., 123: 1269.

Smart, J.S., 1963. Evaluation of exchange interactions from experimental data. In: G.T. Rado and H. Suhl (Editors), Magnetism, volume III. Academic Press, New York, pp.63-114.

Soffel, H., 1977. Pseudo-single-domain effects and single-domain multidomain transition in natural pyrrhotite deduced from domain structure observations. J. Geophys., 42: 351-359.

Sparks, J.T. and Komoto, T., 1964. Etudes de diffraction neutronique à Livermore. J. de Physique, 25: 567.

Sugaki, A., Shima, H., Kitakaze, A. and Fukuoka, M., 1977. Hydrothermal synthesis of pyrrhotites and their phase relation at low temperature. Sci. Rpt. Tohoku Univ., Ser. 3, 13: 165-182.

Takeno, S., 1966. Magnetometric and Röntgenometric studies of pyrrhotite from the Kawayama mine, Japan. J. Sci. Hiroshima Univ., Ser. C., 5: 113-156.

Taylor, L.A., 1970. Low-temperature phase relations in the Fe-S system. Carnegie Institute of Washington Yearbook, 68: 259-267.

Townsend, M.G., Gosselin, J.R., Tremblay, R.J. and Webster, A.H., 1976. Semiconductor to metal transition in FeS. J. de Physique, Colloque C4, 37: 11-16.

Townsend, M.G., Webster, A.H. and Horwood, J.L., 1979. Ferrimagnetic transition in $Fe_{0.9}S$: magnetic, thermodynamic and kinetic aspects. J. Phys. Chem. Solids, 40: 183-189.

Van den Berg, C.B., Van Delden, J.E. and Bouman, J., 1969. α-transition in FeS - a ferroelectric transition. Phys. Stat. Sol., 36: K89-K93.

Vaughn, D.J., Schwarz, E.J. and Owens, D.R., 1971. Pyrrhotites from the Strathcona Mine, Sudbury, Canada: a thermomagnetic and mineralogical study. Econ. Geol., 66: 1131-1144.

Wanic, A., 1964. Magnon scattering of slow neutrons on a pyrrhotite single crystal. J. de Physique, 25: 627-634.

TABLE 1 CURIE-WEISS LAW CONSTANTS

Composition	T_N(K)	θ (K)	C_{mole} (Gcm^3K/oe mole)	$\chi(T_N)$ (Gcm^3/g oe)	References
FeS	593	-917	3.38	$25x10^{-6}$	Hirahara and Murakami (1958)
FeS	613	-857	3.44	-	Chikazumi and Charap (1978, Table 5.1)
FeS	598	-1160	3.74	$25x10^{-6}$	Townsend et al. (1976)
Fe_7S_8	593	-1570	3.44	$17x10^{-6}$	Besnus and Meyer (1964)

TABLE 2 EXCHANGE INTERACTIONS IN Fe_7S_8

(After Marusak, 1979)

Fe site	z_2J_a/k	z_2J_c/k
2	-192K	-204K
4	-192K	-204K
1	-253K	-121K
3	-230K	-130K

TABLE 3 MAGNETOCRYSTALLINE ANISOTROPY CONSTANTS OF 4C MONOCLINIC PYRRHOTITE AT ROOM TEMPERATURE (erg/cm^3)

K_0	K_1	K_2	K_3	K_4	Method	Reference
2×10^5	2.8×10^5	1.0×10^5	7.6×10^6	-	J-H curves up to 25 koe	Besnus (1966)
5.1×10^5	-	-	3.2×10^6	10^5	J-H curves up to 90 koe	Sato et al. (1964)
-	3.5×10^5	$<<K_1$	1.2×10^6	3.2×10^7	J-H curves up to 20 koe	Bin and Pauthenet (1963)
-	2.8×10^5	-	-	-	Torque curves up to 20 koe	Mikami et al. (1959)
-	2.7×10^5	$<<K_1$	-	-	Torque curves up to 20 koe	Hirone et al. (1962)
-	2×10^6	-	2.6×10^6	3.4×10^5	J-H curves up to 100 koe	Adachi and Sato (1968)
-	-	-	2.8×10^6	6.4×10^5	J-H curves up to 100 koe	Sato (1966)

TABLE 4 THERMOMAGNETIC CHARACTERISTICS OF PYRRHOTITES

x	0.000	0.039	0.058	0.077	0.083	0.091	0.092	0.100	0.113	0.127	0.148
Formula	FeS				$Fe_{11}S_{12}$	$Fe_{10}S_{11}$		Fe_9S_{10}		Fe_7S_8	
T_α	145	115	100	80	70	50	-	-	-	-	-
T_S	170	-10	-70	-150	-170	-	-	-	-	-	-
T_H	-	-	110	130	135	150	160	165	165	-	-
T_γ	-	-	150	175	195	215	215	215	220	-	-
T_C	-	-	240	245	250	255	260	260	260+310	310	310
T_β	325	325	325	325	325	325	325	325	325	325	325
$k_{vol} \times 10^6$	60	90	120	110	110	120	140	-	-	-	-
J_s (G)	0	0	0	0	0	0	0	0	65	92	75

Based on data of Schwarz and Vaughn (1972) for samples annealed at 144°C, modified and augmented using data of Haraldsen (1941a), Hihara (1960), Horwood et al. (1976), Marusak (1979) and Townsend et al. (1979). k_{vol} = emu volume susceptibility, J_s = saturation magnetisation (both at room temperature).

Fig. 1 The structure of monoclinic 4C pyrrhotite Fe_7S_8 (after Bertaut, 1953). Alternate iron layers contain vacancies which are ordered as shown. The orthorhombic (4C) unit cell is shown with the sulphur atoms and the complete iron layers omitted for clarity. Iron layers are numbered. There is a slight monoclinic distortion of the orthorhombic unit cell ($\beta = 90.5^{\circ}$), which has space group F2/d. A smaller monoclinic cell (indicated by dashed lines) which has symmetry C2/c and lattice parameters $a=2\sqrt{3}A$, $b=2A$, $c=2C$, $\beta' = 118^{\circ}$ may also be chosen. The hexagonal subcell corresponding to the NiAs (1C) structure is also shown.

Fig. 2 The structures of 4C (Fe_7S_8) and 6C ($Fe_{11}S_{12}$) pyrrhotites, showing all iron layers. The dots indicate iron atoms, open circles denote vacancies and the half-filled circles in the 6C superstructure denote vacancy sites with 50% occupation probability. Magnetic moments of iron atoms in the alternate layers are oppositely directed. Ordering of vacancies onto alternate layers in 4C pyrrhotite produces a nett ferrimagnetic moment as shown. In 6C pyrrhotite the magnetic moments (not shown) of the two sublattices (even and odd Fe layers) cancel. Therefore 6C pyrrhotite is antiferromagnetic.

Fig. 3 (a). Hexagonal unit cell of the NiAs structure on which structures of the pyrrhotite group are based. Closed circles indicate iron atoms, open circles with dots are sulphur atoms. The iron atoms are stacked in identical layers forming hexagonal prisms, each consisting of six trigonal prisms. The sulphur atoms are at the centre of alternate trigonal prisms, which are indicated by shading of the triangular faces. The sulphur layers follow the stacking sequence ABABA...

The unit cell has been expanded to show the atomic arrangement clearly. In fact the atoms are in contact, the sulphurs are arranged in the hexagonal close-packed configuration with the iron atoms occupying all the octahedral interstices.

This structure is known as 1C and is adopted by troilite above about 215°C and by the $Fe_{1-x}S$ solid solution at high temperatures.

3 (b). The central iron atom of 1.1(a), illustrating the 6-fold octahedral (antiprismatic) co-ordination of sulphur atoms about the iron atoms in the 1C structure.

3 (c). The 6-fold prismatic co-ordination of iron atoms about the sulphur atoms in the 1C structure.

Fig. 4 Thermomagnetic (high-or low-field) curve for troilite (FeS) showing knicks in curve at T_α, T_s and T_β (after Schwarz and Vaughn, 1972).

Fig. 5 High-field thermomagnetic curve for Fe_7S_8 and Fe_9S_{10}, showing Weiss-type and peak-type behaviour respectively. Fe_9S_{10} with 5C superstructure is antiferromagnetic at room temperature becomes ferrimagnetic at T_H (~ 170°C), exhibits a thermomagnetic peak at T_γ, and reverts to antiferromagnetism at T_C (after Schwarz and Vaughn, 1972).

Fig. 6 Phase diagram of the central portion of the Fe-S system below 350°C (after Power and Fine, 1976).

Fig. 7 Low-field thermomagnetic (k-T) curves for pyrrhotite classified on the basis of their high-field thermomagnetic (J_s-T) characteristics (see Fig. 2.2).

7 (a) Weiss-type pyrrhotite (monoclinic 4C pyrrhotite).

7 (b) Peak-type pyrrhotite (~Fe_9S_{10}). This diagram is a composite based on several runs with virgin samples. The pronounced thermal hysteresis exhibited by peak-type pyrrhotite is indicated by alternative curves (dashed lines). On heating to above 400°C magnetite is produced, accompanied by a large increase in susceptibility (dotted line).

7 (c) Mixed-type pyrrhotite (a mixture of Weiss-type and peak-type).

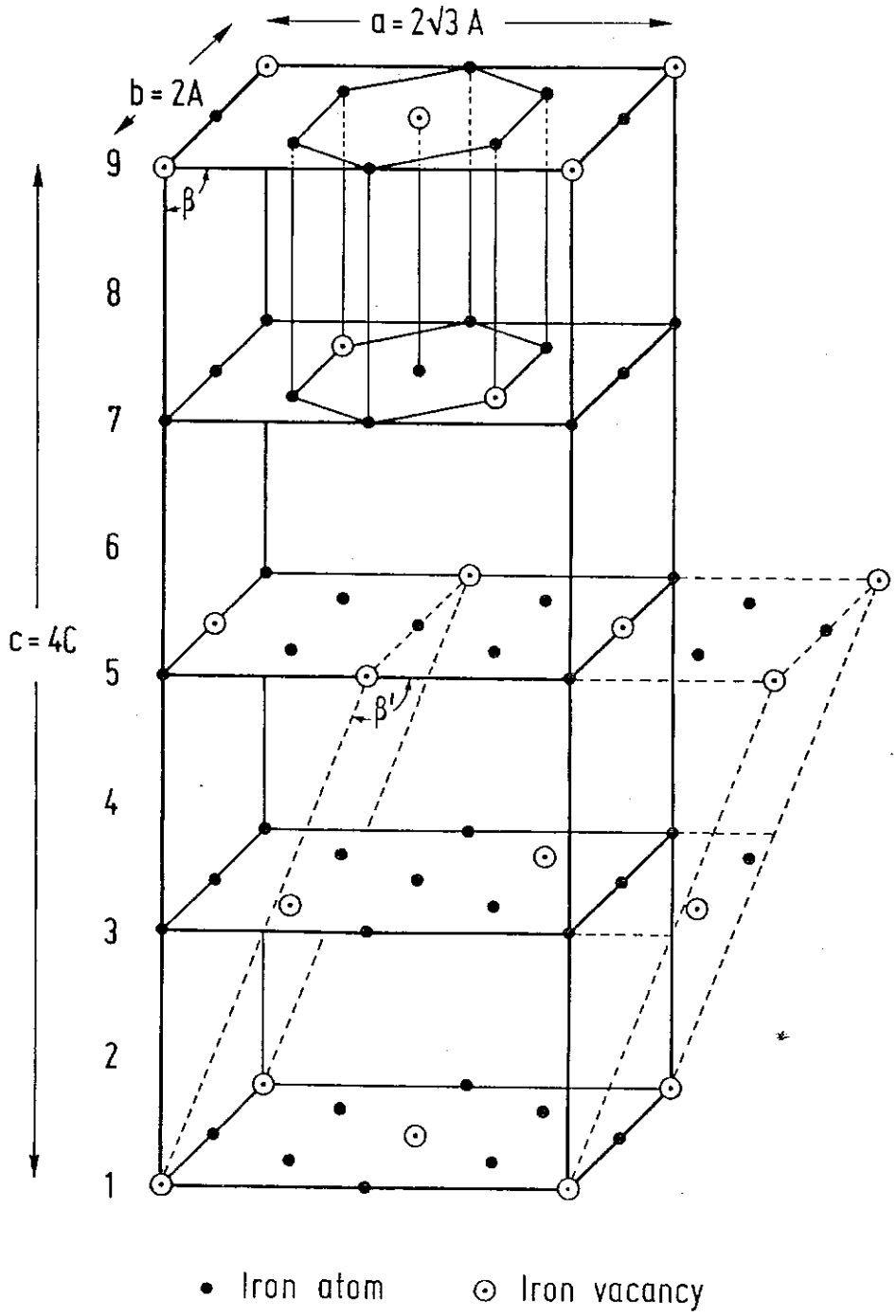

FIG. 1

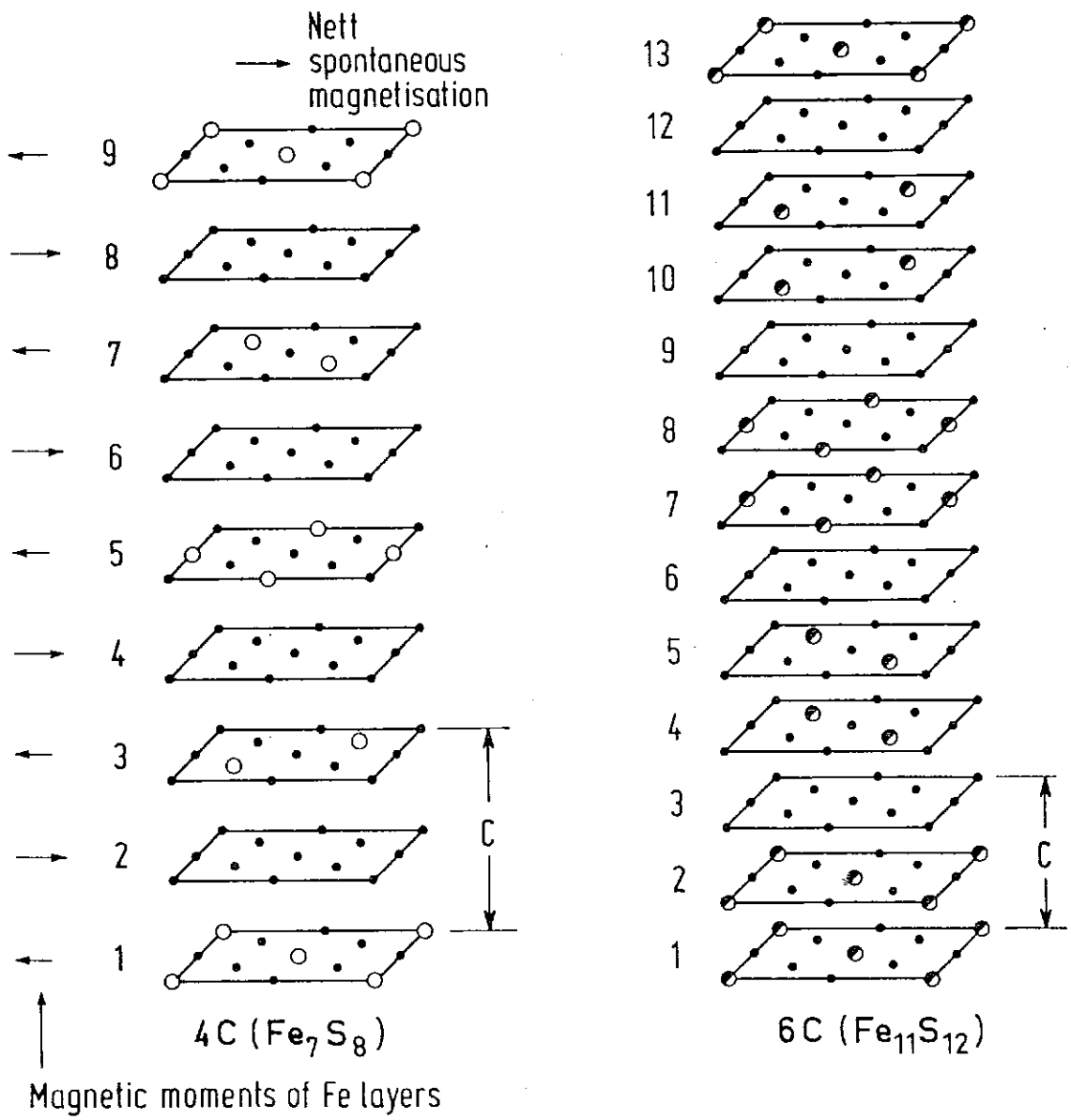
Nett
spontaneous
magnetisation
9
8
7
6
5
4
3
2
1
C
4C (Fe7 S8)
Magnetic moments of Fe layers
13
12
11
10
9
8
7
6
5
4
3
2
1
C
6C (Fe11S12)

FIG.2

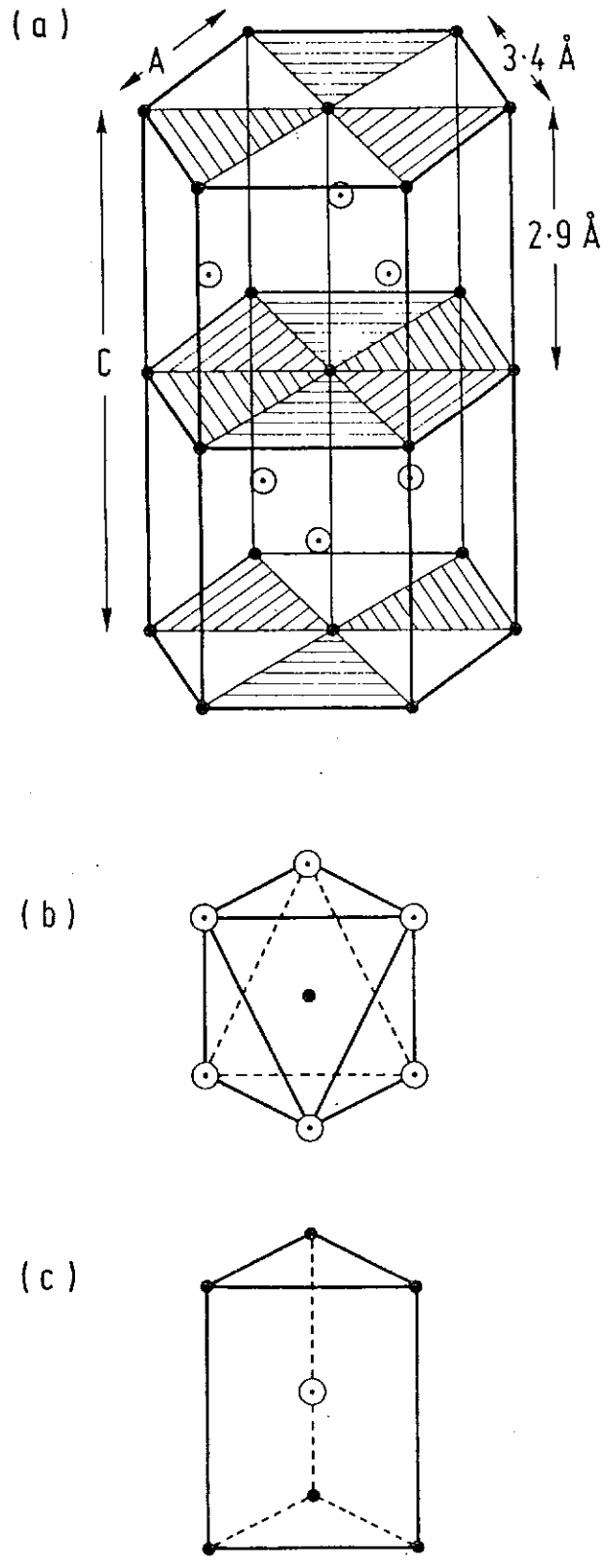

FIG.3

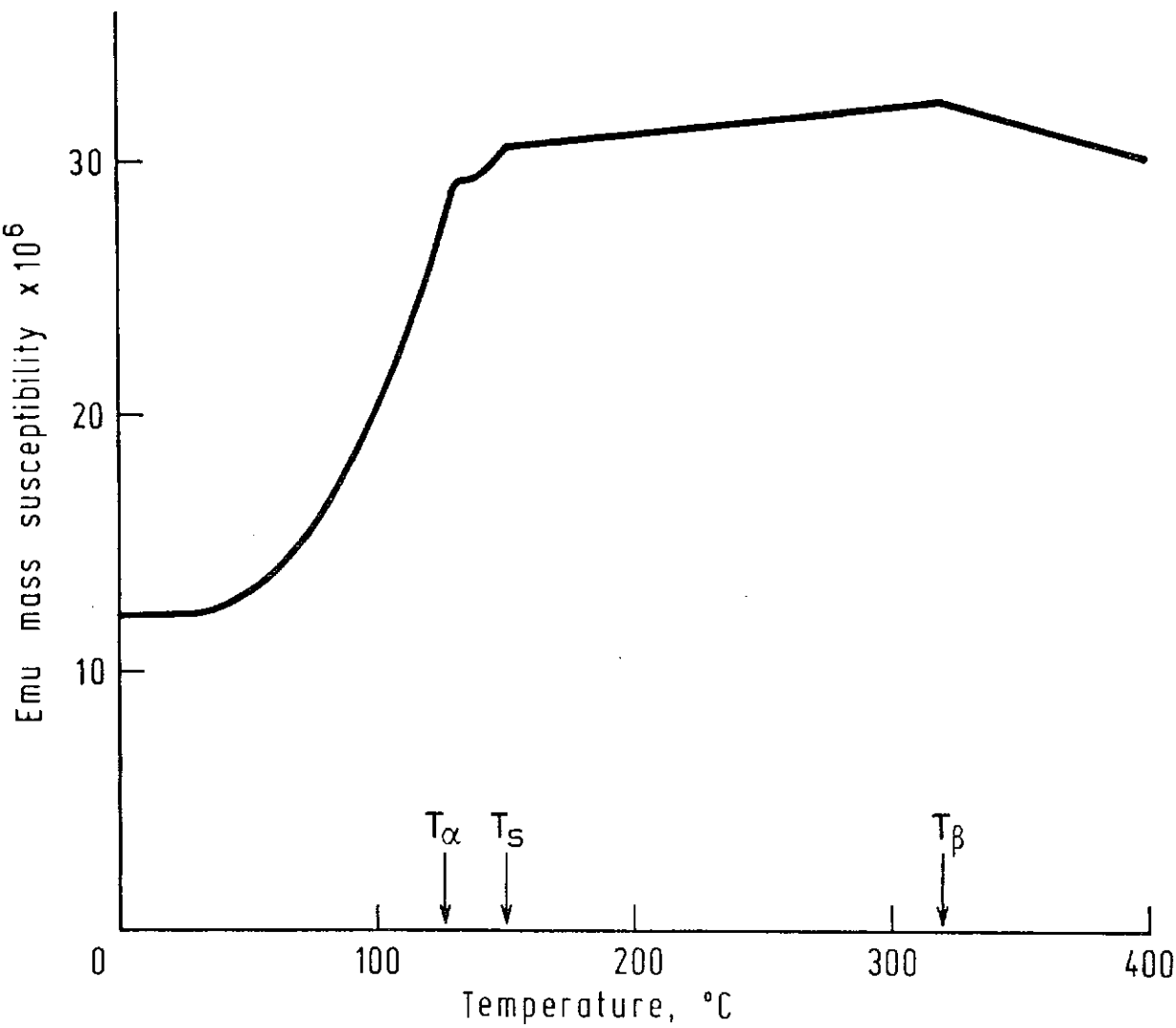
Emu mass susceptibility x 10^6
30
20
10
0
100
200
300
400
Temperature, °C
Tα
Ts
Tβ

FIG.4

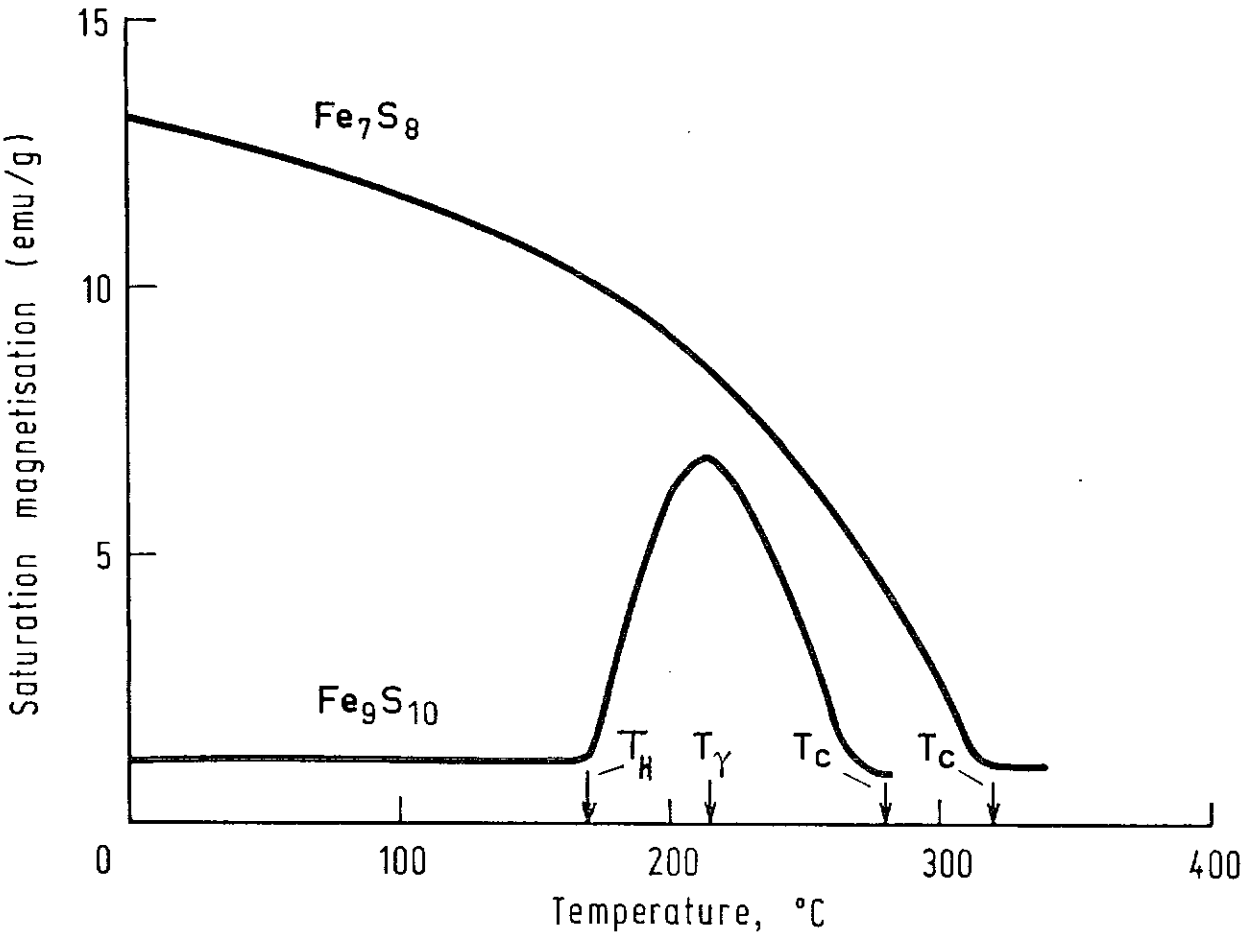
15
10
5
0
100
200
300
400
Saturation magnetisation (emu/g)
Temperature, °C
Fe7S8
Fe9S10
TH
Tγ
TC
TC

FIG.5

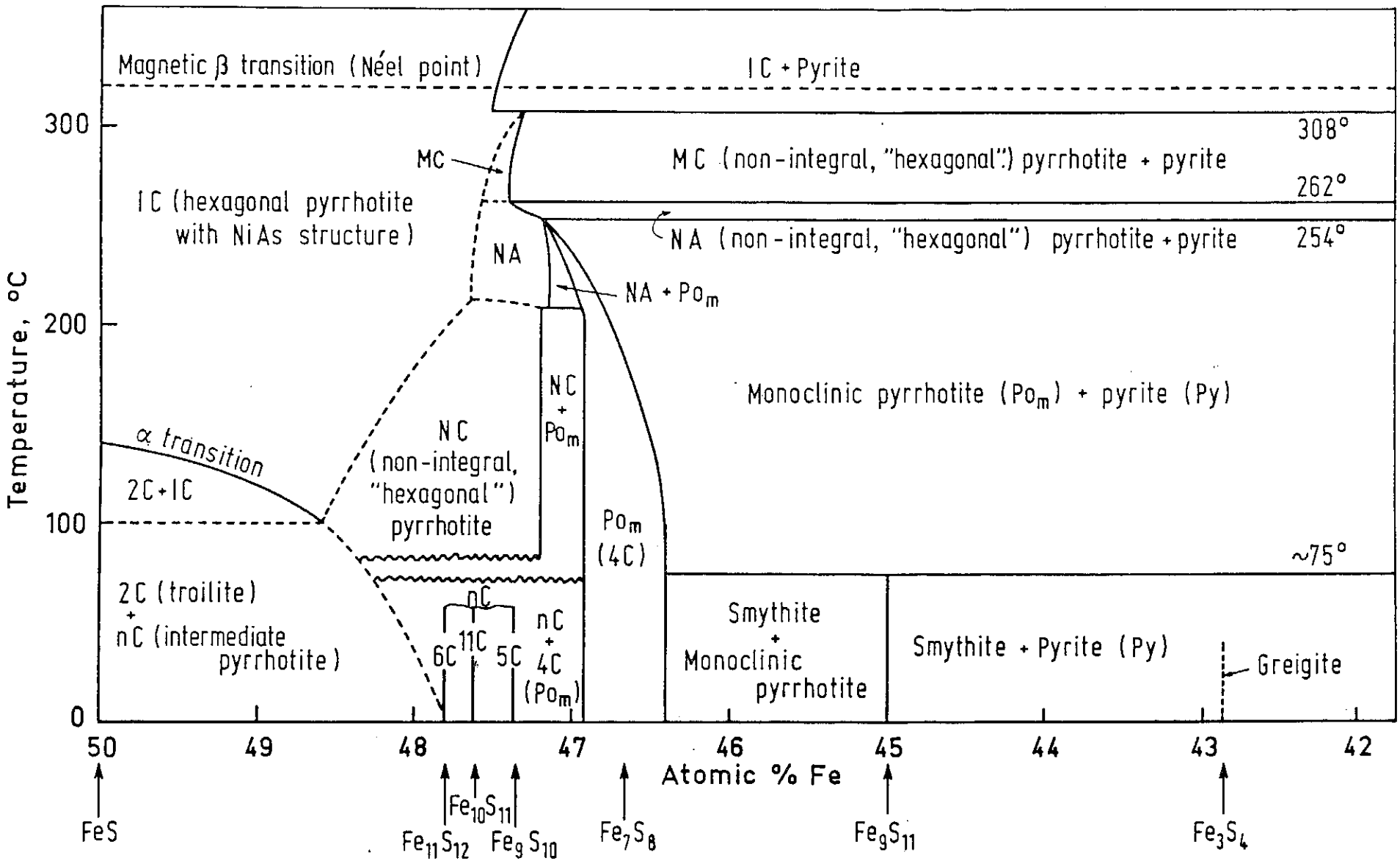
Magnetic β transition (Néel point)
IC + Pyrite
308°
MC (non-integral, "hexagonal") pyrrhotite + pyrite
262°
MC
IC (hexagonal pyrrhotite with NiAs structure)
NA
NA (non-integral, "hexagonal") pyrrhotite + pyrite
254°
NA + Pom
NC + Pom
Monoclinic pyrrhotite (Pom) + pyrite (Py)
α transition
2C + IC
NC (non-integral, "hexagonal") pyrrhotite
Pom (4C)
~75°
2C (troilite) + nC (intermediate pyrrhotite)
nC
6C
11C
5C
nC + 4C (Pom)
Smythite + Monoclinic pyrrhotite
Smythite + Pyrite (Py)
Greigite
Temperature, °C
300
200
100
0
50
49
48
47
46
45
44
43
42
Atomic % Fe
FeS
Fe11S12
Fe10S11
Fe9S10
Fe7S8
Fe9S11
Fe3S4

FIG.6

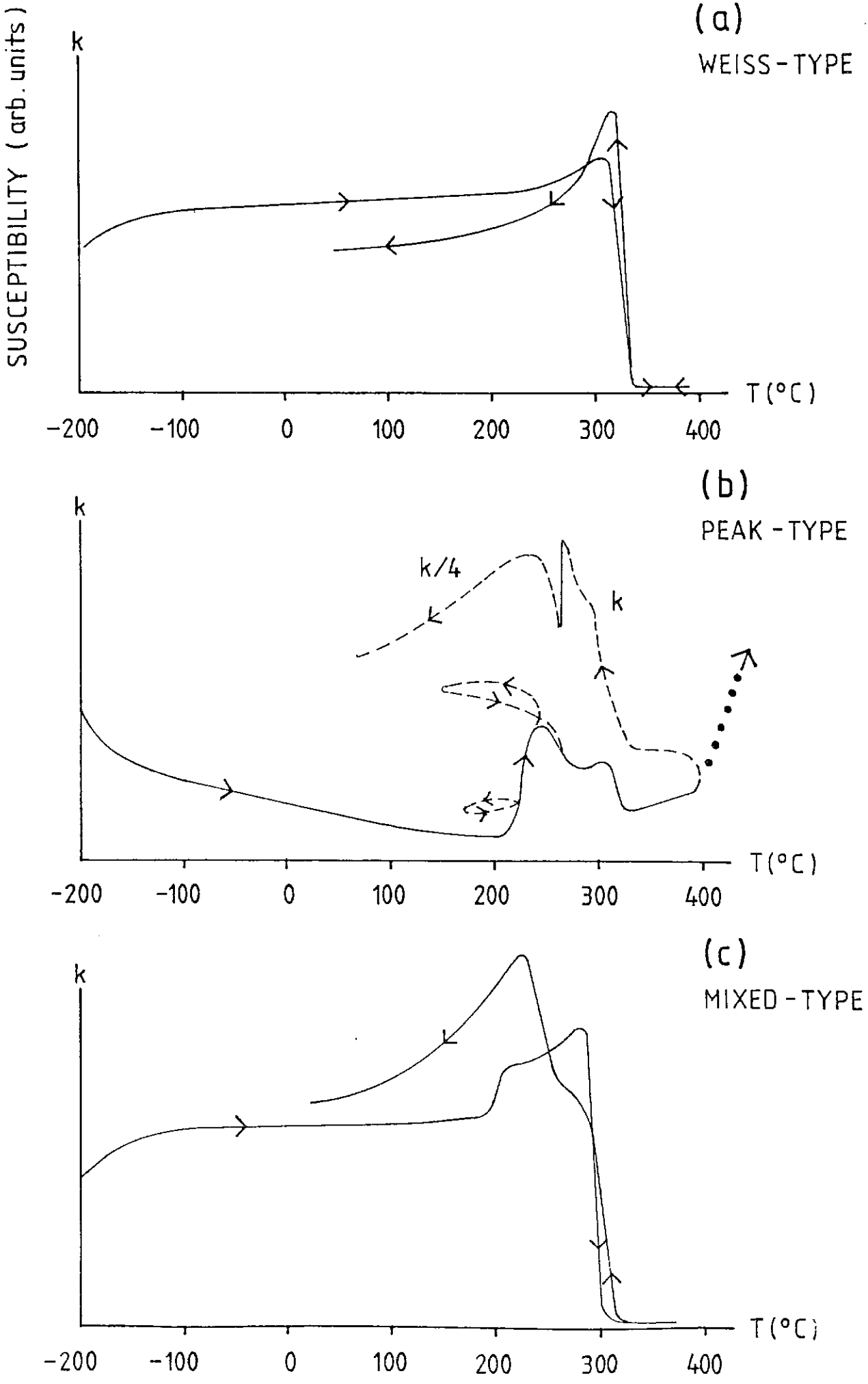
SUSCEPTIBILITY (arb. units)
k
(a)
WEISS-TYPE
T(°C)
-200
-100
0
100
200
300
400
(b)
PEAK-TYPE
k/4
k
(c)
MIXED-TYPE

FIG.7